Eur. Phys. J. D **22**, 189–192 (2003)
DOI: 10.1140/epjd/e2002-00237-5

THE EUROPEAN PHYSICAL JOURNAL D

Regenerative soot as a source of broad band VUV light

Shoaib Ahmad[a]

Accelerator Laboratory, PINSTECH, P.O. Nilore, Islamabad, Pakistan

Received 4 February 2002 / Received in final form 24 September 2002
Published online 17 December 2002 –

Abstract. A mechanism is proposed for the emission of a broad band VUV light to be emitted from the regenerative sooting discharges on the basis of unusually intense intercombination lines of C^+(CII) and C^{++}(CIII) that have been observed. Comparison of these high intensity intercombination lines with the allowed transitions of the highly excited and ionized C constituents of the sooting discharge indicates that one can exploit this mechanism to employ the regenerative soot as a VUV source. The emission of such a broad VUV band from the sooting discharges depends critically on the high energy electrons, metastable gas atoms and C ions trapped by the 3D cusp magnetic field contours.

PACS. 32.70.Fw Absolute and relative intensities – 34.50.Dy Interactions of atoms and molecules with surfaces; photon and electron emission; neutralization of ions – 34.80.Dp Atomic excitation and ionization by electron impact

A mechanism for the emission of enhanced, broad band VUV light by the highly excited levels of the singly, doubly and triply charged C ions from the regenerative sooting discharge [1] is presented. We have observed intense intercombination lines from the carbon vapour that is produced and trapped in cusp magnetic field contours. The intercombination multiplets and lines of C^+(CII) and C^{++}(CIII) at λ = 2324–8 Å (the 233 nm multiplet) and λ = 1908 Å, respectively, have very small Einstein transition probabilities. Therefore, these ions have to be trapped for significantly longer times $\sim$ ms with high energy ($\geq$ 10 eV) electrons for excitation to the levels responsible for transitions that we observe. The entrapment ensures multiple collisions with energetic electrons that excite the ions and also increase ions' charge. The second significant stage is the de-excitation of the highly charged C ions by the radiative and dielectronic recombinations. These ions eventually de-excite to the ground or the first excited states either directly or *via* recombination-cascades. The first excited states of CII and CIII are heavily populated with the subsequent intercombination transitions to the respective ground levels.

Intercombination lines have been observed among the emissions from astrophysical objects like planetary nebulae [2], cool stars [3] and in the solar chromosphere [4] because the rate of collisional excitations and deexcitations of ions in these astrophysical objects and diffuse plasmas are of the same order of magnitude as the radiative decay rates for the metastable levels. The intensity ratios involving forbidden and the allowed lines are electron density and temperature sensitive. For this reason the emissions from the metastable levels have served as important electron density n_e and temperature T_e diagnostics [2–4]. Evaluation of n_e has been done for a broad range of T_e from the relative intensities of the allowed and forbidden transitions of CIII emissions from quasi-stellar objects (QSO) [5]. The spectroscopic studies of the allowed emission lines of CII–CIV have served as an important tool for the investigations of divertor-plasma impurities [6–9]. Typically, in these tokamak plasmas one deals with rather high electron densities $n_e \sim 10^{13}$–10^{15} cm^{-3} and ratios of only the allowed transitions of CII, CIII and CIV have been used for the effective electron temperatures for the respective species. The range of n_e in various astrophysical situations is from 10^5 to 10^{12} cm^{-3}. The ratio of CII levels yielding the intercombination (λ = 2324–8 Å) and allowed (λ = 1335 Å) multiplets of CII has also been explored [10,11] for T_e = 10,000 K to 32,000 K as a function of n_e. This ratio reduces significantly with increasing n_e and collisional deexcitations play dominant role for $n_e \geq 10^{12}$ cm^{-3}.

The most significant aspect of our carbonaceous discharges produced in the regenerative soot in a specially designed hollow cathode is that these are initiated and sustained by the two well defined electron energy regimes [12]; the first regime has energies $\geq$10 eV and the other with $\leq$1 eV. The high energy electrons ($\geq$10 eV) are emitted from the graphite cathode, accelerated by the transverse electric field in the cathode dark space and are trapped by the $E \times B$ and $B \times \nabla B$ fields along the extended cusp magnetic field contours. These trapped electrons ionize the support gas (He or Ne) whose metastable atoms in turn sputter the cathode to introduce C content into the plasma. These C atoms are similarly excited and ionized giving carbonaceous character to the initially pure noble gas discharge. The positive column of the

[a] e-mail: shoaib@pinstech.org.pk

discharge fills the entire hollow cathode has a large number of metastables of Ne and C atoms and ions with excitation temperature $T_{\rm exc} \leq 1$ eV and electron density $n_{\rm e} \sim 10^{10-12}$ cm^{-3} [13]. The role of hexapole magnetic field contours that extend along the entire hollow cathode cavity is crucial to the generation of the two electron energy regimes and a C dominated noble gas discharge. Electrons with $E \geq 10$ eV ensure high probability of the multiply charged carbon C^{n+} ($n \geq 1$) and noble gas ions. The entrapment of the carbonaceous discharge in the cylindrical hollow cathode by the 3D cusp field contours serves in three important ways; (1) in the cusps and near the cathode walls the trapped high energy electrons with $E \geq 10$ eV ensure higher probabilities of the multiply charged C^{n+} ($n \geq 1$), (2) it provides a positive column of high density of low energy electrons ($T_{\rm exc} \leq 1$ eV) for the excitation and recombination processes and (3) its role in the electronic de-excitation of the first excited states is such that it does not produce significant non-radiative collisional de-excitation. The above mechanisms help to create C vapour having long lived excited states of the trapped ions. Five to six orders of magnitude intense intercombination lines of CII and CIII compared with the allowed radiative transitions have been observed in our experiments. The predominant mechanism for the densely populated first excited states is by the de-excitations of the highly excited ions. Among the by-products are the autoionization states and Rydberg states of the neutral and the ionized C. The de-excitations of these states can yield a strong, broad band VUV radiation field between 200–1000 Å *i.e.*, $E_{\rm photon}$ between 50 and 20 eV.

The schematic diagram of the source in the inset of Figure 1 shows the inter-penetrating, graphite Hollow Cathode and Anode. The hexapole, cusp magnetic field is generated with six bar magnets. A cut away radial cross-section of the source shows the intersection of the field lines with the graphite cathode surface. These magnetic contours are curved 3D surfaces extending along the z-axis. Detailed description of the source and its sooting characteristics is provided in references [13]. Figure 1 shows two spectra taken with Ne at 0.1 mbar, $i_{\rm dis}$ = 200 mA but at different discharge voltages; Figure 1a is with $V_{\rm dis}$ = 0.6 kV while in Figure 1b $V_{\rm dis}$ = 1.5 kV. 20 NeI emission lines are identifiable between λ = 5500–6500 Å that decay to the first excited states. Therefore, we have a large fraction of the metastable Ne atoms which is an efficient potential sputtering agent for the regeneration of the soot [14]. Two excited atomic lines of CI at λ = 1931 Å and λ = 2478 Å are the signatures of the cathode sputtering and for the generation of a carbonaceous discharge. The graphite hollow cathode discharge with Ne as the source gas shows two distinct groups of emission lines between 180 and 650 nm. The first group is between 180–250 nm. This includes emission lines of the neutral, singly, doubly and triply charged carbon denoted as CI, CII, CIII and CIV. The second distinct and high intensity group of NeI emission lines lies between 580–650 nm. An enlarged view of the wavelength region between 180–250 nm is also shown in the inset of Figure 1a.

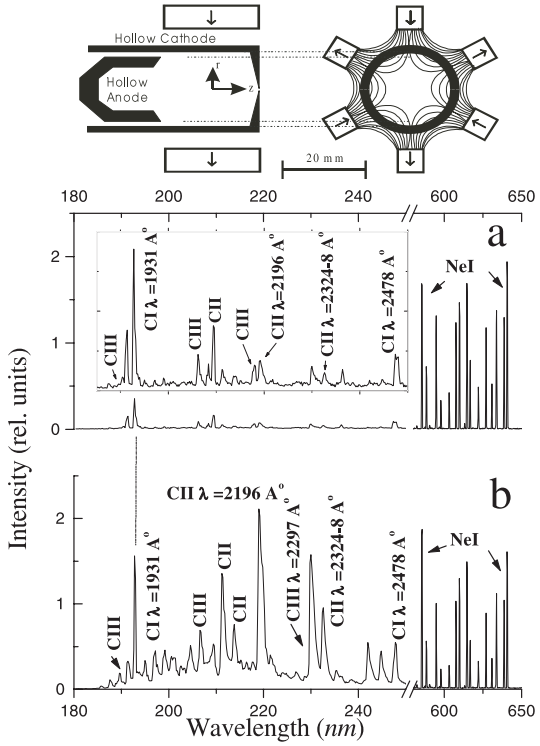

Fig. 1. The experimental set up of the source shows the interpenetrating graphite Hollow Cathode and Hollow Anode. A cross-sectional view of the hexapole,cusp magnetic field is also shown. Photoemission spectra is presented with Ne as the support gas at two different discharge voltages with $P_{\rm g} \approx 0.6$ mbar, $i_{\rm dis}$ = 200 mA being kept constant. For (a) $V_{\rm dis}$ = 0.6 kV and (b) $V_{\rm dis}$ = 1.5 kV. The relative lines intensities are plotted against the wavelength. The x-axis is broken in the two wavelength ranges of 180–250 nm and 550–650 nm, respectively. Inset in (a) shows the CI, CII and CIII lines enlarged by a factor of 5.

An unusual and intense intercombination line of CII at λ = 2196 Å is also pointed with an arrow. This enlarged CII peak at $V_{\rm dis}$ = 0.6 kV is 40 times smaller than the one shown in Figure 1b. In Figure 1b the discharge voltage increased to $V_{\rm dis}$ = 1.5 kV. All the respective peaks of CI, CII, CIII and CIV seen in Figure 1a are also enhanced as shown in Figure 1b but the magnitude of enhancement is lower for the excited neutral carbon CI as compared with the ionized C. Highly excited and charged carbon vapour is the active ingredient of the graphite hollow cathode discharge with enhanced sputtering at higher values of $V_{\rm dis}$. We will particularly discuss CII's 233 nm multiplet. The CII λ = 2196 Å transition has high intensity for this spin forbidden transition $2p^2\ {}^2{\rm S}_{1/2}$–$2p^3\ {}^4{\rm S}_{3/2}$ that has transition probability $\simeq 5.1\ {\rm s}^{-1}$. The lines and multiplets are interpreted by using NIST's Atomic Database available on the web [15].

From the relative intensities of the emission lines, we have tabulated the respective upper level densities for the five chosen transitions in Figure 2. These transitions include CII, CIII intercombination transitions at

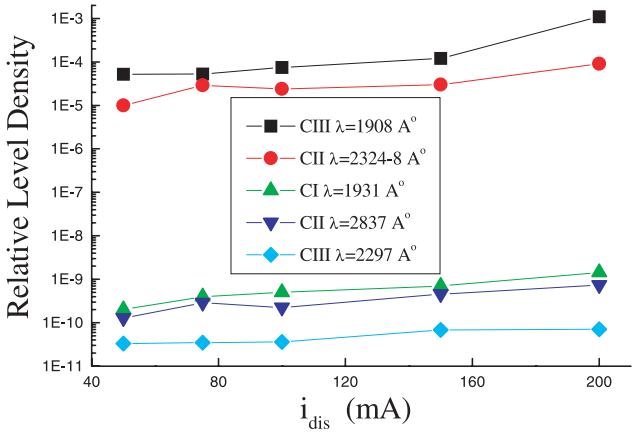

Fig. 2. From the relative intensities of the emission lines, the respective upper level densities for the five chosen transitions are tabulated and presented . These transitions include the two CII and CIII intercombination transitions at $\lambda = \lambda 2324$–8 Å (*i.e.*, the 233 nm multiplet) and $\lambda = 1908$ Å and the allowed transitions $\lambda = 2837$ Å and the $\lambda = 2297$ Å. A CI line at $\lambda = 1931$ Å is also plotted.

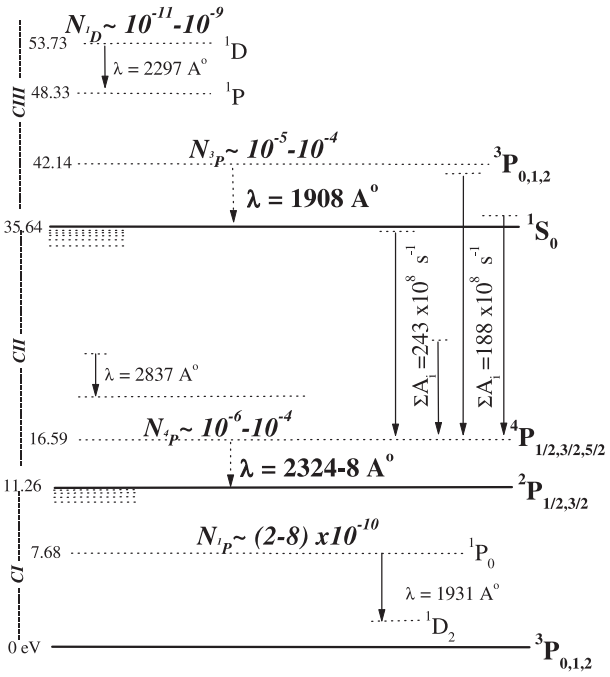

Fig. 3. The energy levels diagram of CI, CII and CIII shows representative transitions and the calculated relative number densities of the respective levels. The allowed as well as the intercombination lines are indicated. The cumulative sum of the Einstein transition probabilities ΣA_i of the total number of the possible transition to the first excited states of CII are shown. Unbroken arrows show the allowed and the dotted lined arrows are for the intercombination transitions.

$\lambda = 2324$–8 Å (*i.e.*, the 233 nm multiplet) and $\lambda = 1908$ Å and the allowed transitions $\lambda = 2837$ Å and the $\lambda = 2297$ Å. One CI line at $\lambda = 1931$ Å is included to identify and highlight the mechanism of ionization of the sputtered C atoms by energetic electrons in the cusp magnetic fields. The respective level densities in the figure indicate the CI $3s\ ^1P^0$ ($\lambda = 1931$ Å), CII $2p^2\ ^4P$ (233 nm) and $3p\ ^2P^0$ ($\lambda = 2837$ Å) and for CIII $2p\ ^3P^0$ ($\lambda = 1908$ Å), $2p^2\ ^1D$ ($\lambda = 2297$ Å). The relative level densities are plotted as a function of the discharge current $i_{\rm dis}$ at constant Ne pressure $P_{\rm Ne} = 0.1$ mbar. There are at least six orders of magnitude differences between the term densities leading to the intercombination lines and the allowed ones. We see that the 233 nm multiplet representing a highly populated $2p^2\ ^4P$ term. It has also been observed that the densities of all the CII and CIII excited levels reduce as the pressure is increased. The collisional processes or the radiationless transitions may be dominant at higher pressures. However, the two intercombination transitions are 6–7 orders of magnitude more intense compared with the allowed transitions.

Figure 3 shows an energy levels diagram of CI, CII and CIII that has been prepared to show some of the observed and discussed transitions and the calculated number densities of the respective levels. The allowed as well as the intercombination lines are indicated. The cumulative sum of the Einstein transition probabilities ΣA_i of the total number of all possible transition to the first excited states of CII are also indicated. Unbroken arrows show the allowed and the dotted ones the intercombination transitions. This energy levels diagram has been constructed in such a way so that the state of excitation of CI, CII and CIII can be illustrated. We have also shown the range of the relative number densities of respective states. It is these number densities that provide the crucial information regarding the mechanisms of the electron induced excitation, ionization and recombinations of this unique carbonaceous discharge. The plasma boundaries of this discharge are defined by the cusp magnetic field contours where electrons and C ions are trapped. Here the electrons have high kinetic energies $K.E. \geq 10$ eV and act as efficient ionization agents [16] while the ions have low $K.E. \sim T_{\rm e} \leq 1$ eV but high potential energies ∼12–60 eV. Movement along the extended magnetic field contours ensures that the electronic motion is randomized and a Maxwellian velocity distribution is approached. Collisions can be radiative as well as dielectronic. The ionic motion is governed by their charge and the ambient electric field directed towards the cathode. The magnitude of the electric field will determine their final $K.E.$ with which they strike the cathode and contribute to the recycling of the soot into the discharge by kinetic as well as potential sputtering. By varying $i_{\rm dis}$, $P_{\rm g}$ and the type of the support gas our results have shown that: (1) a large number of lines from the neutral, singly and doubly ionized C are emitted along with the discharge gases' characteristic lines. A significant number of CII lines can be observed that originate both from within the autoionization levels and the excited levels above the first excited state ^4P. (2) The intense 233 nm multiplet is seen in all the spectra with high intensity although it has very small transition probabilities for all five lines of the multiplet $\simeq 2.14 \times 10^2\ {\rm s}^{-1}$. This multiplet is generally a weak intersystem transition route for

the de-excitation of CII in diffuse interstellar clouds [17]. From the energy levels scheme and using NIST's Atomic Database [15], we know that a total of 14 CII multiplets are emitted by de-excitation of the quartet terms to ^{4}P. This in turn de-excites to the ground term ^{2}P by the emission of the 233 nm multiplet. Its intense emission indicates that CII exists as a highly excited C ion in the discharge. (3) The CII intercombination line at $\lambda = 2196$ Å is the other most unusual feature that indicates a high level density for the $2p^3\ ^4S_{3/2}$. Its intensity has direct proportionality to $i_{\rm dis}$ and varies inversely with the gas pressure. As shown in Figure 1 $\lambda = 2196$ Å line is the main emission line observed in He discharge. Its dominant presence indicates that resonant electron collisional as well as photon absorption mechanisms are operative.

Exploitation of this unique carbonaceous discharge is proposed that is composed of a positive column whose outer boundaries are defined by the cusp magnetic field contours to operate as a source of enhanced VUV light and soft X-rays. These contours confine and trap high energy electrons and low energy C ions. The graphite hollow cathode acts as a cavity that traps the charged species whose radiative decay can yield a strong VUV radiation field that exists between $\lambda = 20$–80 nm. Figure 4 has been prepared in the form of a histogram in which the cumulative Einstein transition probabilities ΣA_i of the three charged states of C are plotted as a function of the wavelength. This field has a broad peak between 30–70 nm. The main contributions to this field are the radiative and dielectronic recombinations of CII, CIII and CIV. When all three ionized states are present then three distinct regimes of wavelength exist; (a) below 40 nm, emission from CIV dominate ($E_{\rm photon} \sim 40$ eV), (b) between 40–60 nm emissions from CIII dominate ($E_{\rm photon} \sim 25$ eV), and (c) above 60 nm, emissions from CII dominate ($E_{\rm photon} \leq 20$ eV). The increased population densities of the metastable levels indicate the existence of broad emission bands comprising lines and multiplets due to the multiply ionized C. The entrapment of the C ions along the cusp magnetic fields and their subsequent collisions with energetic electrons that are similarly trapped but gyrate with different frequencies is the essence of this mechanism. The light that is predicted from such a source will emit broad band peaked between 20–80 nm. It works with a medium that comprises of the radiative and dielectronic transitions between the entire energy level scheme of CI to CIV (and possible CV as well). The lower temperature discharge contained between the cusp fields acts as the source of the excited C atoms and ions. Once the full potential of the above described mechanism is recognized, there are number of important fields where this mechanism may be effectively utilized. The above mechanism can provide a possible route to the generation of soft X-rays laser [18] directly or as a pumping source, for example.

This work is an outgrowth of the indigenous work on the regenerative soot and the author gratefully acknowledges the support of colleagues in the Charged Particle Accelerator Lab. at PINSTECH, Islamabad, Pakistan.

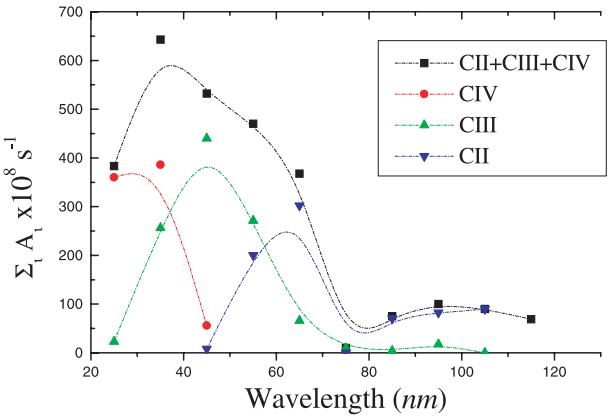

Fig. 4. A histogram is plotted for the cumulative transition probabilities of CII, CIII and CIV as a function of the wavelength λ. The total of ΣA_i for (CII+CIII+CIV) is also drawn. The wavelength interval for the histogram is chosen as $\Delta\lambda = \pm 10$ nm.

References

1. The mechanisms and processes leading to the Regenerative Soot have been discussed in a recent review article: S. Ahmad, Eur. Phys. J. D **18**, 309 (2002)
2. F.P. Keenan, W.A. Feibleman, K.A. Berrington, Ap. J. **389**, 443 (1992)
3. R.E. Stencil *et al.*, Mon. Not. R. Astr. Soc. **196**, 47P (1981)
4. H.E. Mason, Phil. Trans. R. Soc. Lond. A **336**, 447 (1991)
5. M. Loulerge, H. Nussbaumer, Astron. Astrophys. **51**, 103 (1976)
6. H. Kubo *et al.*, Nucl. Fusion **33**, 1427 (1993)
7. C.F. Maggi *et al.*, J. Nucl. Mat. **241-243**, 414 (1997)
8. R.C. Isler *et al.*, Phys. Plasmas **4**, 355 (1997)
9. K. Lee, D.E. Kim, Phys. Rev. E **60**, 2224 (1999)
10. M. A. Hayes, H. Nussbaumer, Astron. Astrophys. **134**, 193 (1984)
11. D.J. Lennon, P.L. Dufton, A. Hibbert, A.E. Kingston, Ap. J. **294**, 2090 (1985)
12. H. Falk, *Improved Hollow Cathode lamps for Atomic Spectroscopy*, edited by C. Sergio (Ellis Horowood, Chichester, 1985), Chap. 4
13. S. Ahmad, T. Riffat, Nucl. Instrum. Meth. Phys. Res. B **152**, 506 (1999); S. Ahmad, Eur. Phys. J. AP **5**, 111 (1999); S. Ahmad, Phys. Lett. A **261**, 327 (1999)
14. S. Ahmad, M.N. Akhtar, Appl. Phys. Lett. **78**, 1499 (2001)
15. NIST Atomic Spectra Database (ADS) Data at `http://physics.nist.gov/`
16. Using semi-empirical formulation for ionization rate coefficient α_i given by W. Lotz, Ap. J. **14**, 207 (1967); we obtain for $E_{\rm electron} \geq 10$ eV, $\alpha_i \sim 10^{-8}$ to 10^{-12} cm^3 s^{-1} for producing CII, CIII and CIV from their respective ground states. On the other hand for $E_{\rm electron} \sim 1$ eV α_i is between 10^{-13}–10^{-37} cm^3 s^{-1} for producing the same ionic states
17. Th. Henning, F. Salama, Science **282**, 2204 (1998)
18. A. Zerikhin, K. Koshelov, Sov. J. Quant. Mech. **6**, 82 (1976); P. Hegelsten, Plasma Phys. **25**, 1345 (1983); U. Feldman, A. Bhatia, S. Suckewer, J. Appl. Phys. **54**, 2188 (1983); J. Zhang *et al.*, Phys. Rev. Lett. **74**, 1335 (1995)